The SCOPE Dynamic Model for Emulsion Polymerization I. Theory

EUGENE P. DOUGHERTY, *Research Laboratories, Rohm and Haas Company, P. O. Box 219, Bristol, Pennsylvania 19007*

Synopsis

The SCOPE dynamic process model has been developed to treat batch and semibatch emulsion copolymerizations. This computer-based model treats jacketed reactors of arbitrary size. It consists of a coupled set of ordinary differential and algebraic equations that describe material balances for the reacting species and energy balances for both the reactor and the cooling water jacket. The model also includes a feature that allows for proportional integral derivative (PID) control of the monomer emulsion and cooling water feed rates to a reactor temperature set point. The model is based largely upon the kinetic theories developed by Smith, Ewart, and Harkins to treat emulsion homopolymerizations. The SCOPE model improves upon and expands the classic theories by taking advantage of recent theoretical developments in emulsion polymerization. Such phenomena as diffusion-controlled termination and radical desorption—important for predicting accurate polymerization rates—are included in the model. More modern theories of particle nucleation, including both homogeneous and micellar mechanisms, have been incorporated into the model to predict accurate particle size distributions. SCOPE also extends the classic theories to treat the emulsion copolymerization of an arbitrary number of monomers. Output from the model includes species concentrations, residual monomer levels, particle size distributions, molecular weight distributions, instantaneous and cumulative copolymer compositions, and reactor temperatures as a function of time. The SCOPE model can be used to evaluate various process control strategies and to study the effects of process dynamics on polymer properties. In Part II, SCOPE model predictions are compared with experimental data for styrene-methyl methacrylate copolymerizations.

INTRODUCTION

Since the 1940s, there have been major research efforts to understand the process of emulsion polymerization. In 1947, Harkins[1] developed a reasonable qualitative model, stating that emulsion polymerization is a free-radical polymerization process that takes place in particles generated by soap "micelles." Smith and Ewart[2] cast the Harkins model in the form of equations, which were then solved by methods developed by Stockmayer[3] and O'Toole.[4] The Smith-Ewart-Harkins model was reasonably successful in describing the details of the emulsion polymerization of styrene.[2] In the 1960s, Gardon[5] and Uglestad et al.[6] reformulated and extended the Smith-Ewart-Harkins model, concentrating on such details as diffusion-controlled termination, concentration of monomer in the particles, and radical desorption from particles. By 1970, emulsion polymerization theory was well established, at least for water-insoluble monomers.

Priest[7] and Baxendale et al.[8] interpreted experiments with water-soluble monomers using theories different than those proposed by Smith, Ewart, and Harkins. Later experiments with methyl methacrylate, carried out by

Journal of Applied Polymer Science, Vol. 32, 3051–3078 (1986)
 CCC 0021-8995/86/013051-28$04.00

Roe[9] and Fitch et al.,[10] confirmed that particles could be generated in the absence of soap (i.e., without micelles), at least for slightly water-soluble monomers. Still other experiments[11] indicated clearly that the rate of polymerization does not follow the dependence on soap and initiator concentration predicted by the Smith, Ewart, and Harkins models. Therefore, Roe[9] and Fitch et al.[10] developed models with homogeneous particle nucleation mechanisms, which modified the prevailing Smith-Ewart-Harkins picture considerably.

Although early models of emulsion polymerization focused only upon the emulsion kinetics, recent researchers have coupled the reaction kinetics with the reactor dynamics. Min and Ray[12] and the Hamielec and MacGregor research groups at McMaster[13] have developed detailed, computer-based models that treat the polymerization kinetics as well as the reactor dynamics. Such models indicate how the process dynamics influences polymer properties.

This paper describes the SCOPE (simulation and control of polymer emulsions) computer-based dynamic process model. The SCOPE model draws heavily upon the ideas of the researchers mentioned above to describe typical industrial batch or semibatch emulsion copolymerizations. The user supplies the SCOPE computer program with the emulsion recipe, such process conditions as flow rates and temperatures, and kinetic parameters, such as rate constants and reactivity ratios. The SCOPE model then calculates species concentrations, particle size, and molecular weight as a function of time. Since SCOPE includes processing and equipment parameters as well as the emulsion chemistry, the model is similar in spirit to models developed by Ray[12] and Hamielec and MacGregor.[13] The SCOPE model, on the other hand, simplifies the more detailed models of Refs. 12 and 13 by using simpler correlations and fewer parameters. Furthermore, SCOPE uses a new algorithm for computing particle size distributions. Finally, it extends previously developed models to treat emulsion copolymerization recipes involving an arbitrary number of monomers.

The SCOPE model was designed to treat batch and semibatch (i.e., semicontinuous or gradual addition) emulsion copolymerizations, although a continuous version of the model has been developed as well.[14] Figure 1 is a diagram of the system being modeled by SCOPE. The species considered in the model include the following: water (or other diluent), one or more monomers, (co)polymer, soap, initiator, promoter, activator, and/or chain transfer agent. Some (or all) of these species may be present in the starting reaction mixture, or some (or all) may be added to the reactor as a monomer emulsion feed stream, in which case the monomers polymerize as they are fed in. The pronounced exothermicity characteristic of emulsion polymerizations requires some means of heat removal for large-scale processes. The SCOPE model assumes that reactor cooling is effected by means of a cooling water jacket. The reactor temperature is maintained at a set point by using PID control, where either or both the monomer emulsion flow rate and the cooling water flow rate are the manipulated variables.

The present paper outlines the theoretical equations underlying the SCOPE model. First, material and energy balance equations as well as the associated proportional integral derivative (PID) control equations are presented for the system pictured in Fig. 1. Next, the reaction chemistry of

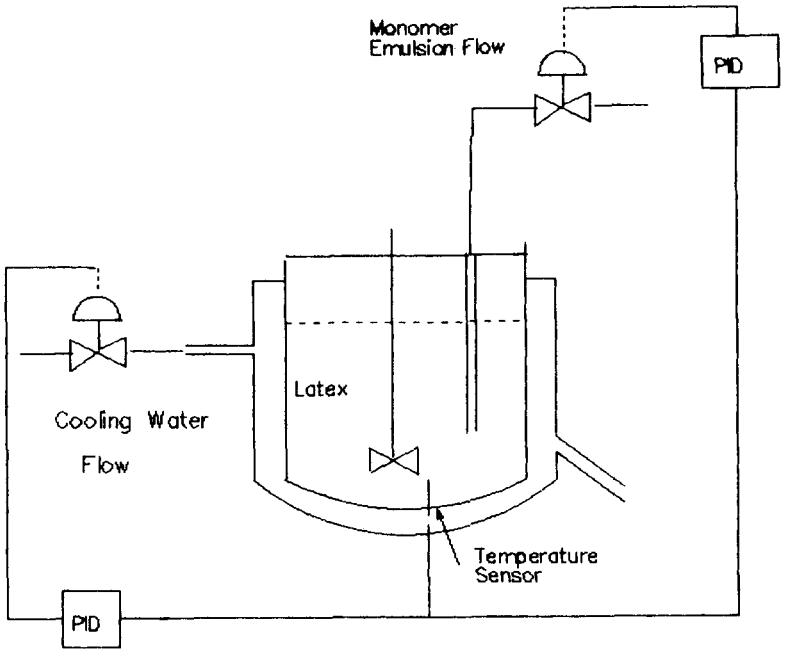

Fig. 1. Diagram of the system modeled by SCOPE. PID denotes a proportional integral derivative controller, which controls feed rates of monomer emulsion and cooling water in order to maintain the temperature near some desired set point.

emulsion copolymerization is discussed. Mathematical expressions relate the reaction kinetics and process variables to conversion, species concentrations, molecular weight, particle size, and copolymer compositions. In part II, the results of the SCOPE model are compared with some relevant experimental results, and some potential applications of the model are illustrated. SCOPE gives very good agreement with several experiments reported by Nomura et al. for styrene-methyl methacrylate copolymerization.[15]

THEORY

Material and Energy Balances

Material balance equations are developed for the total reactor volume (1), the total amount of monomer added (2), soap (3), initiator (4), activator (5), promoter (6), chain transfer agent (7), copolymer (8), the number of particles (9), and each of the m monomers in the system (10). The glossary explains notation.

$$\frac{d}{dt} V_l = F_{ef} - \left(\frac{1}{\rho_m} - \frac{1}{\rho_p}\right) V_l \sum_{i-1}^{m} R_{p_i} M_i \qquad V_l(0) = V_i \tag{1}$$

$$\frac{d}{dt} [M_{ta}] V_l = F_{ef} [M_{ta}]_{ef} \qquad [M_{ta}](0) = [M_{ta}]_i \tag{2}$$

$$\frac{d}{dt}[S]V_l = F_{ef}[S]_{ef} \qquad [S](0) = [S]_i \tag{3}$$

$$\frac{d}{dt}[I]V_l = F_{ef}[I]_{ef} - k_d[I]V_l \qquad [I](0) = [I]_i \tag{4}$$

$$\frac{d}{dt}[A]V_l = F_{ef}[A]_{ef} - R_A V_l \qquad [A](0) = [A]_i \tag{5}$$

$$\frac{d}{dt}[C]V_l = F_{ef}[C]_{ef} - R_C V_l \qquad [C](0) = [C]_i \tag{6}$$

$$\frac{d}{dt}[T]V_l = F_{ef}[T]_{ef} - R_T V_l \qquad [T](0) = [T]_i \tag{7}$$

$$\frac{d}{dt}N_p V_l = Np_{\text{gen}} V_l \qquad N_P(0) = N_{p_i} \tag{8}$$

$$\frac{d}{dt}[P]V_l = V_l \sum_{i=1}^{m} R_{p_i} M_i \qquad [P](0) = [P]_i \tag{9}$$

$$\frac{d}{dt}[M_1]V_l = F_{ef}[M_1]_{ef} - R_{p_1} V_1 \qquad [M_1](0) = [M_1]_i \tag{10a}$$

$$\vdots \qquad \vdots \qquad \vdots \qquad \vdots \qquad \vdots$$

$$dt[M_m]V_l = F_{ef}[M_m]_{ef} - R_{p_m} V_l \qquad [M_m](0) = [M_m]_i \tag{10f}$$

Several points about these equations should be clarified. First, initial conditions (reactor conditions before the monomer emulsion is fed in) must be specified. Second, eq. (1) includes a term to account for the shrinkage in volume due to conversion of monomer to polymer (which always occupies less specific volume). Third, the reaction rate expressions in these equations (e.g., R_{p_i}) have not been specified yet: the section Process Control will explain how to calculate these rates. Finally, all quantities appearing in eqs. (1) through (10) could be time dependent. Although this dependence is not explicitly shown, all quantities are updated while these differential equations are integrated forward in time.

Using eqs. (2) and (10) we calculate the current weight conversion according to

$$X = \frac{[M_{ta}] - \sum_{i-1}^{m} M_i [M_i]}{[M_{ta}]} \tag{11}$$

Equation (1) uses the average monomer density ρ_m and the average copolymer density ρ_p. The model uses weighted averages for such physical properties as densities, monomer molecular weights, and heat capacities. These mass-weighted averages are calculated using

$$\mathbf{P} = \sum_{i=1} w_i p_i^{(0)} \tag{12}$$

Here w_i is the weight fraction of component i and $p_i^{(0)}$ is the ith pure

component property value, so **P** is the general weighted-average property (density, molecular weight, heat capacity, and so on). A particular quantity set in bold type denotes that it has been averaged. The summation in eq. (12) extends over all relevant components in the emulsion feed *ef*, the latex *l*, or the initial charge *i*.

Energy balances are written for both the emulsion reactor and the cooling water jacket. The energy balance for the reactor is

$$\begin{aligned} \frac{d}{dt}\left[\rho_l \mathbf{C}_{p_l}(\mathrm{T}_l - T_{\mathrm{ref}})V_l\right] &= F_{ef}\,\rho_{ef}\mathbf{C}_{p_{ef}}(T_{ef} - T_{\mathrm{ref}}) \\ &\quad - UA_h(T_l - T_w) + V_l \sum_{i=1}^{m} R_p M_i\,\Delta Hp_i \\ [\rho_l \mathbf{C}_{p_l}(T_l - T_{\mathrm{ref}})V_l](0) &= [\rho_i \mathbf{C}_{p_i}(T_i - T_{\mathrm{ref}})V_i] \end{aligned} \tag{13}$$

The heat balance around the cooling water jacket is

$$\begin{aligned} \frac{d}{dt}(\rho_w C_p T_w V_w) &= F_w \rho_w C_p (T_{w_{\mathrm{in}}} - T_w) \\ &\quad - UA_h (T_w - T_l), \qquad T_w(0) = T_{w_i} \end{aligned} \tag{14}$$

The heat transfer area A_h is calculated by

$$A_h = \frac{\pi}{4} d_r^2 + \frac{4V_l}{d_r} \tag{15}$$

where d_r is the reactor diameter. The cooling water volume V_w is calculated assuming that the reactor is cylindrical and that the jacket covers the base and the sides; then,

$$V_w = \frac{\pi}{4} d_r^2 t_w + \pi h_r \left[\left(\frac{d_r}{2} + t_w\right)^2 - \left(\frac{d_r}{2}\right)^2\right] \tag{16}$$

Where t_w is the cooling water jacket thickness and h_r is the reactor height.

Process Control

The computer-based SCOPE model can be used to rapidly evaluate a variety of potential process control strategies. Once the model parameters have been estimated reasonably well for a particular process, SCOPE can be used to evaluate effects of feed temperatures, feed compositions, and flow rates on concentration profiles, polymerization rates and/or final properties. In this manner one can choose a set of operating conditions to keep a process under control.

In SCOPE, a special set of process control equations implements a general control strategy often adopted for emulsion polymerization processes: main-

taining the reactor at specified set-point temperature. Temperature control ensures smooth processing and controls molecular weight development. Feedback control of the monomer emulsion and/or cooling water flow rates is carried out with a standard proportional integral derivative control algorithm.[16] In this procedure either flow rate is related to the valve stem position, which extends from 0 to 100% (fully closed to fully open). PID control changes the valve stem position.

Consider first that the measured temperature may lag behind the actual latex temperature according to a first-order delay equation

$$\frac{d}{dt} T_{\text{meas}} = \frac{T_l - T_{\text{meas}}}{\tau_{\text{meas}}} \qquad T_{\text{meas}}(0) = T_s \tag{17}$$

Where T_{meas} is the time constant of the measuring device. The normalized deviation between the set-point and measured temperature is

$$e = \frac{T_{sp} - T_{\text{meas}}}{T_{\text{meas}}} \tag{18}$$

As stated above, manipulating the monomer emulsion and/or cooling water flow rates maintains small temperature set-point deviations [the e in eq. (18)] and in turn provides good quality and process control. The so-called velocity form of the usual PID equation (16) accomplishes this temperature control by computing a difference Δ_x to be applied to the current controller output:

$$\Delta_x = C_{x_t} - C_{x_{t-1}} = \frac{100}{P_x}[(e_t - e_{t-1}) + I_x e_t + D_x(e_t - 2e_{t-1} + e_{t-2})] \tag{19}$$

Here e_{t-1} and e_{t-2} refer to the deviations evaluated at the previous two time steps. Equation (19) requires that the differential equation method used to integrate the material and energy balance equations evaluate the solution at equally spaced time intervals. The general index x indicates which flow is manipulated by PID control; it may either be the cooling water w or the monomer emulsion feed ef (or perhaps both). The controller constants P_x, I_x, and D_x can be "tuned" using the SCOPE model for particular valves and processes. Naturally, the proportional band constant P_x is negative for the monomer emulsion feed and positive for the cooling water feed.

Once the controller outputs C_{ef} and C_w have been computed using eq. (19), the corresponding valve stem positions S_{ef} and S_w are calculated using first-order delay equations like eq. (17):

$$\frac{d}{dt} S_x = \frac{C_x - S_x}{\tau_x} \qquad S_x(0) = S_{x_0} \tag{20}$$

Here τ_x represents the time lag between a change in controller output and a change in the corresponding valve stem position. In the model the vol-

umetric flow rates F_{ef} and F_w are related to the valve stem positions by interpolation using a table of F_x versus S_x for the particular type of valve used.

Emulsion Polymerization Kinetics

Solution of the material and energy balance equations requires that the reaction rates (e.g., R_{p_i}) be known. Here mathematical expressions will be developed for these reaction rates as well as for the particle size, molecular weight, and copolymer composition. These product quality indicators are determined from knowledge of the polymerization rates and solution of material and energy balance equations.

Let us first review the generally accepted qualitative model of emulsion polymerization. Many researchers[1,2,5,6,13,17] view emulsion polymerization as a process consisting of three distinct intervals (see Fig. 2). In interval I, the particle nucleation stage, particles are produced by either one of two mechanisms: micellar particle generation or homogeneous particle generation. Homogeneous particle generation occurs when radicals begin to polymerize in the aqueous phase. Polymerization continues in the aqueous phase until a critical length is reached and particles are formed by precipitation. Very small particles can rapidly undergo "microcoagulation"[18] to form larger polymer particles, which usually have to be at least 100 Å in diameter to be colloidally stable. In micellar particle generation, radicals "sting" micelles, which are collections of soap molecules, to form new particles, where polymerization then starts. Interval I ends when the soap concentration

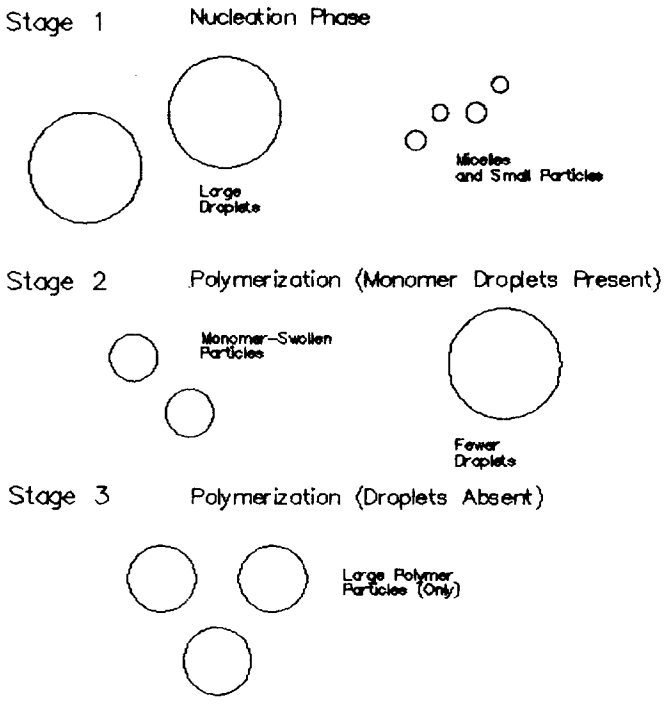

Fig. 2. The three stages of emulsion polymerization.

becomes sufficiently low that no particles are generated (all the soap is required to stabilize particles that have already formed). Interval I is generally short: particle generation is usually completed at low (<5%) conversion. As Fig. 2 shows, in interval II both large monomer droplets (approximately 1–10 μm) as well as polymer particles (approximately 0.02–1.00 μm) are present. In this interval, polymerization progresses as monomer from the droplets rapidly diffuses into the polymerizing particles. Monomer droplets are present because the monomers are not completely soluble in the polymer particles: the increase in surface free energy required to swell the particles is too high. Interval II ends when these droplets disappear; that is, enough monomer polymerizes to permit all remaining monomer to stay in the particles. Usually this occurs around 40% conversion. In interval III polymerization continues, often at an accelerated rate. This occurs because polymer chains become sufficiently entangled to cause the termination reaction to become diffusion controlled and thus orders of magnitude slower. Propagation takes place more rapidly relative to termination, until it, too, finally becomes diffusion controlled at very high (usually about 98%) conversion.

Although this three-interval picture strictly applies to a batch emulsion polymerization, the model described above may be used to understand semibatch or continuous processes as well. The polymer chemistry literature usually uses the same kinetic treatment for all three types of processes.[12,13,19] To be sure, process parameters as well as the reaction kinetics will dictate what happens at a particular instant. Thus, the meaning of "interval" is less clear, because mechanisms ordinarily associated with one interval may be occurring at the same time as those associated with a different interval. For instance, for semibatch or continuous processes, new particles may be nucleated even as particles produced earlier are simultaneously growing out. The resulting particle size distribution will reflect these competing processes.

Initiation

In emulsion polymerization initiation is either dissociative (thermal) or chemical (redox). Usually, dissociative initiators are persulfates, which dissociate at high temperature and exhibit first-order kinetics:

$$I(S_2O_8^{-2}) \xrightarrow{k_d} 2R^{\cdot}\,(SO_4^{-\cdot}) \tag{21}$$

where k_d is the initiator decomposition rate constant. The rate of thermal initiation is

$$R_I = 2fk_d[I] \tag{22}$$

The radical efficiency factor f, which usually has a value between 0.5 and 1.0, accounts for the fact that not all persulfate radicals initiate polymeric radicals.

Mechanistically, the thermal initiation process is believed to occur according to the following scheme[17,20]:

$$\begin{aligned} S_2O_8^{2-} &\rightarrow 2SO_4^{-}\cdot \\ SO_4^{-}\cdot + H_2O &\rightarrow HSO_4^{-} + OH\cdot \\ 2OH\cdot &\rightarrow H_2O + \frac{1}{2}O_2 \end{aligned} \tag{23}$$

Experimental measurements indicate that the efficiency of initiation is lower at higher persulfate concentrations because of a "cage effect"[17,20] in which radicals quench each other. Moreover, initiation efficiency is weakly dependent on ionic strength and pH and influenced by side reactions with other species present in emulsion polymerizations (e.g., mercaptans).[17,20-22] The SCOPE model does not include every mechanistic detail, but instead it uses an "effective" radical efficiency factor f to incorporate these effects:

$$f = f_0\left(1 - a_1 \ln \frac{[I]}{[I_0]}\right) \tag{24}$$

In eq. (24) f_0 is the nominal efficiency factor determined at some reference concentration $[I_0]$. Experiments carried out at different initiator concentrations are used to determine the parameter a_1.

Redox initiation is a more complex process, and in many cases the mechanistic details need to be determined by an appropriate kinetic study.[17] Still, many redox-initiated polymerizations can be represented in two steps.[19] In step 1 a promoter (usually a ferrous salt) reacts with an initiator (persulfate or peroxide) to produce primary radicals by an oxidation-reduction process:

$$C^{+a} + I \xrightarrow{k_{r1}} C^{+a+b} + R^{\cdot} + \text{other products} \tag{25}$$

In a second important step, the ferrous ion is regenerated by an oxidation-reduction reaction with an activator (e.g., sodium metabisulfite or sodium sulfoxylate formaldehyde):

$$C^{+a+b} + A \xrightarrow{k_{r2}} C^{+a} + A' \tag{26}$$

The initiation rate for many redox processes is given by[22]

$$R_I = fk_{r_1}[C^{+a}][I] = fk_{r_1}\frac{k_{r_2}[C][A]}{k_{r_1}[I] + k_{r_2}[A]} \tag{27}$$

The total promoter concentration $[C]$ and the activator concentration $[A]$ are calculated by the appropriate material balance equations (6) and (7). Equation (27) assumes that C^{+a} rapidly attains a steady-state concentration

[see eqs. (25) and (26)]. If this occurs, initiation is pseudo-first-order [i.e., eq. (27) becomes similar to eq. (22)].

Propagation

Once primary radicals have been generated, chain propagation can take place in the polymer particles:

$$M + -R_r^{\cdot} \xrightarrow{k_p} -\mathrm{R}_{r+1}^{\cdot} \tag{28}$$

Here $R_r^{\cdot}$ denotes a propagating free radical chain length r. The propagation rate constant—as well as all other rate constants used in the SCOPE model—are assumed to be independent of polymer chain length. The rate constants, however, exhibit temperature dependence of the usual Arrhenius form

$$k_x = A_x \exp\left(-\frac{E_x}{RT}\right) \tag{29}$$

According to eq. (25), the rate of propagation (polymerization) is

$$R_p = k_p[M_p]\,[M\cdot] \tag{30}$$

since all propagation is assumed to take place within the polymer particles. Equation (30) is valid for a single monomer. For copolymers, a different propagation rate constant applies for each monomer-radical pair. I will treat propagation of more than one monomer in a later section on copolymer composition.

Monomer Concentration in the Particles

The concentration of monomer in the particles must be determined in order to compute the propagation rate. The introduction to this section noted that small emulsion particles can become saturated with monomer during interval II of polymerization. A saturation monomer concentration is reached when the loss in free energy due to mixing monomer with polymer is matched by the gain in interfacial free energy caused by swelling small polymer particles with monomer. Thus, thermodynamics dictates the concentration of monomer in the particles. Thermodynamic equilibrium is quickly reached and maintained in emulsion polymerizations[17] because of rapid diffusion of monomer through the aqueous phase.

The particle size and the chemistry of the monomer (or monomers) and polymer (or copolymer) determine the concentration of monomer in the polymer particles. The partitioning of each monomer in the polymer and aqueous phases should be determined over the entire particle size range of interest. Morton et al.[23] and Kriegbaum and Carpenter[24] have formally derived the equations for determining the partitioning of monomers in copolymers over the typical ranges of emulsion particle sizes, but these equations involve interaction parameters that are not usually known. Oishi

and Prausnitz[25] have used the UNIFAC approach[25,26] with some success in calculating this partitioning for complex solubilities, but, as yet, accurate parameters are not available for many important chemical functionalities, so exact calculations are out of the question at the present time.

Fortunately, the parameter x_c, which is approximately the conversion at which the monomer droplets disappear, has been tabulated for many common monomers. With this parameter a simple material balance on the total monomer allows us to calculate the saturation monomer concentration $[M_p]_{sat}$[13]

$$[M_p]_{sat} = \frac{a_2 \rho_m}{\mathbf{M}_w} \frac{1 - \mathbf{x}_c}{1 - \mathbf{x}_c \left(1 - \frac{\rho_m}{\rho_p}\right)} \tag{31}$$

In eq. (31), $\mathbf{M}_w$ is the average monomer molecular weight, ρ_p the density of the (co)polymer, and ρ_m the monomer density. The parameter a_2 is usually equal to 1, but for certain highly water-soluble monomers, it may be less than 1. This parameter, which takes into account the partitioning of the monomer in the aqueous phase, can be estimated from experiments that carefully determine the partitioning of monomer in the droplet phase, polymer particles, and the aqueous phase.

After interval II, when the monomer concentration becomes sufficiently low that the monomer droplets disappear, the model assumes that all the monomer is in the polymer particles; then,

$$[M_p] = \frac{[M]V_l}{V_p} \quad \text{when} \quad [M_p]_{sat} > \frac{[M]V_l}{V_p}$$
$$[M_p] = [M_p]_{sat} \quad \text{otherwise} \tag{32}$$

In eqs. (32), $[M]$ is the total concentration of monomer in the latex and V_p is the total volume of the particles (both can be calculated by solving the material balance equations).

A rigorous calculation of the monomer concentration in the particles for copolymers requires knowledge of how the monomers interact with each other as well as with the copolymer. According to MacGregor and Hamielec,[13] however, one can assume without appreciable error that the monomers distribute themselves in the same molar proportions in the aqueous, polymer particle, and monomer droplet phases. Evidence suggests that this remains valid even for copolymers formed by monomers with very different water solubilities. For instance, Fordyce and Chapin[27] have shown that styrene-acrylonitrile copolymer composition profiles are almost identical in both emulsion and bulk polymerizations. In view of this, SCOPE simply solves the material balance equations for each monomer (10) to get the residual monomer compositions and assumes these compositions remain the same in all phases. Equations (31) and (32) are used to calculate the total monomer concentrations in the particles. Mass-weighted averages are used in eq. (31) for the monomer molecular weights, the monomer and copolymer densities, and the $\mathbf{x}_c$ parameter.

Average Number of Radicals per Particle

To compute the radical concentration $[M\cdot]$ used in eq. (27), we consider both the number of particles per liter N_p and the average number of radicals per particle $\bar{n}$:

$$[M\cdot] = \frac{\bar{n}N_p}{N_a} \tag{33}$$

The rates of initiation, termination, and chain transfer determine the average number of radicals per particle. Primary radicals formed in the aqueous phase via initiator decomposition can rapidly diffuse into polymer particles and undergo chain propagation reactions. Alternatively, radicals may terminate by either combination or disproportionation:

$$-R_r^{\cdot} + -R_q^{\cdot} \begin{cases} \xrightarrow{k_{tc}} P_{r+q} \\ \xrightarrow{k_{td}} P_r + P_q \end{cases} \tag{34}$$

The overall termination rate constant k_t is equal to $k_{tc} + k_{td}$.

It is well known[28-30] that the termination rate becomes diffusion controlled in high-conversion free-radical polymerizations. Since the polymerization occurs in small polymer particles, at high conversions the polymer concentrations are such that chain entanglements and reduced free volume significently reduce the mobility of macroradicals. The termination rate decreases significantly, increasing the average number of radicals per particle, which in turn increases the polymerization rate. The deGennes reptation theory[28] and free volume theory[29,30] have been invoked to describe this phenomenon, although both of these approaches rely on a number of adjustable parameters to fit the available experimental data. The most common approach taken in modeling this so-called gel effect is to assume that the termination rate constant falls with increasing conversion (or decreasing free volume).[13] Following the lead of Ref. 31, the SCOPE model uses a simple, empirical (yet asymptotically correct) formula that uses only two parameters to track the decrease in termination with increasing conversion:

$$k_t = \frac{k_{t_0}}{1 + a_3 X^{a_4}} \tag{35}$$

Where k_{t_0} is the value of the termination rate constant at zero conversion. The parameters a_3 and a_4 are determined by kinetic experiments that span the range of conversion from 0 to 100%. This expression fits the forms developed for the more sophisticated treatments[12,28-30] quite well. At extremely high (approximately 98%) conversion, the propagation rate can also become diffusion controlled.[12,29,30] This happens when the polymerization temperature exceeds the glass temperature T_g of the polymerizing mixture. In certain systems where this occurs in progressing (e.g., α-methyl

styrene), an expression similar to eq. (35) can be used for the propagation rate constant. As a general rule, however, the decrease in propagation rate constant occurs at such a high conversion that SCOPE gives satisfactory agreement with experiment without the need for special propagation rate constant-conversion correlations.

The average number of radicals per particle can also be affected by chain transfer reactions; that is,

$$-R_r^{\cdot} + T \xrightarrow{k_{tr\text{-}T}} P_r + T^{\cdot} \tag{36}$$

Unlike termination reactions, however, chain transfer reactions per se do not decrease the number of radicals per particle. However, if transfer to monomer or to another small molecule occurs, the number of radicals per particle can decrease because the smaller radicals so formed can more easily diffuse out of the polymer particles and then terminate in the aqueous phase before being reabsorbed. Naturally, the radical desorption rate is somewhat dependent upon the particle surface area: the rate of desorption is greater in those particles with a large surface area to volume ratio (i.e., small particles). Following the suggestion of Uglestad et al.,[6,32] SCOPE accounts for the effect of surface area by using a single radical desorption rate parameter k'_{de} to calculate the average number of radicals per particle.

Smith and Ewart[2] have examined the processes of initiation termination and desorption. By assuming that the radicals rapidly establish a steady state, they have developed a recurrence equation for calculating the number of radicals per particle. Stockmayer[3] showed that the solution to this recurrence equation involved Bessel functions, and O'Toole[4] explained why a particular form of the Bessel function provided an acceptable solution. Smith and Ewart[2] and, later, Uglestad et al.[6,32] have examined the behavior of the recurrence equation for the number of radicals and have arrived at equations for three limiting cases. These general cases encompass virtually all emulsion polymerizations. Since detailed derivations of these equations are available elsewhere,[6,13,33] I simply summarize the results and present the formulas for the average number of radicals per particle below used in SCOPE.

Vinyl acetate[33] and vinyl chloride exhibit case I kinetics. For these monomers, chain transfer of radicals to monomer, subsequent desorption from the particles, and termination in the aqueous phase proceed quickly relative to propagation. Not surprisingly, then, the average number of radicals per particle depends on the termination rate constant, the desorption rate constant, the particle size, and, of course, the initiation rate R_I. The general expression is

$$\bar{n}_I = N_a \left[\frac{R_I}{N_p} \left(\frac{v_p}{2k_t} + \frac{v_p^{2/3}}{2k'_{de}} \right) \right]^{1/2} \tag{37}$$

Typically, $\bar{n}_I$ is much less than 1 for case I emulsion polymerizations.

Case II kinetics applies to low-conversion emulsion polymerizations of many monomers, including styrene and many acrylic monomers. In case

II polymerizations, radical desorption and water-phase termination rates are negligible compared with the radical entry rate into the particles. However, the radical termination rate in the polymer particles occurs on the same time scale as the radical entry rate. Therefore, half the time each particle will contain one radical and half the time none at all (termination within the particles is virtually instantaneous). Therefore, $\bar{n}_{II} = 0.5$.

Case III kinetics applies to high-conversion polymerizations when termination becomes diffusion limited and transfer reactions are slow relative to propagation. The expression for the average number of radicals per particle is similar to that of eq. (37):

$$\bar{n}_{III} = N_a \left(\frac{R_I v_p}{2 N_p k_t} \right)^{1/2} \tag{38}$$

Multiplying this equation by the particle concentration gives an expression for radical concentration very similar to that derived for bulk or solution polymerizations. At very high conversions, where the termination rate becomes very slow relative to the initiation rate, $\bar{n}_{III}$ can be as high as 100 for certain case III systems.

Number of Particles per Liter

The concentration of radicals is a product of the average number of radicals per particle and the number of particles per liter [eq. (33)]. In some semibatch emulsion polymerizations, polymer particles are added at the beginning (before the monomer emulsion is fed in). Soap concentrations are often deliberately maintained at low levels to ensure that no new particles are generated. When polymer is present initially, the initial particle concentration is calculated by dividing the polymer concentration by the weight of an average polymer particle:

$$N_p = \frac{6[P]}{\pi \, d_p^3 \, \rho_p} \tag{39}$$

If the soap concentrations are sufficiently low that no new particles are generated, then the polymer particles added at the beginning simply grow out uniformly to produce a monodisperse particle size distribution. The particle concentration decreases slightly by a dilution factor as the latex volume increases.

This paper has already mentioned the controversy reported in the polymer chemistry literature[7-11,18,33] concerning mechanisms for particle generation in emulsion polymerizations. Older theories of Harkins[1] and Smith and Ewart[2] contended that particles were generated by a heterogeneous mechanism wherein collections of soap micelles were stung by primary radicals formed in the aqueous phase. On the other hand, experiments with slightly water-soluble monomers at low soap levels[7-10] indicate that particle generation can occur by a homogeneous mechanism whereby radicals polymerize to a certain critical length in the aqueous phase and then finally

precipitate as particles.[8-11] Lichti et al.[18] have presented convincing experimental evidence that very small polymer particles formed by aqueous phase initiation usually microcoagulate[18] to form larger, more stable polymer particles with diameters ranging from about 50 to 300 Å.

The expression used in the model for $N_{p_{gen}}$, the particle generation rate, assumes that particles could be generated by either a micellar mechanism or by a homogeneous mechanism, or perhaps by both pathways concurrently:

$$N_{p_{gen}} = R_I N_a \frac{\zeta A_m + \mu}{\zeta A_m + \mu + \gamma \zeta A_p} \tag{40}$$

Equation (40) is a simplified version of an expression originally suggested by Kiparissides et al.[33] The expression from Ref. 33 is rather involved, including radical desorption and parameters describing the homogeneous particle nucleation rate. Equation (40) "lumps" several of these parameters into two: an effective homogeneous nucleation rate parameter μ and the radical capture of parameter γ. As Ref. 33 suggests, these parameters can be estimated from conversion and particle size distribution measurements.

Let us examine eq. (40) in detail. Regardless of whether particles are generated by micellar or homogeneous nucleation, the generation rate is proportional to R_I, the rate of initiation. The effective rate of homogeneous nucleation depends on several physicochemical factors. Water-soluble monomers with low colloidal stability have a high value of the parameter μ; strongly hydrophobic monomers with high colloidal stability would have a low value. The product $\gamma \zeta A_p$ represents the rate of radical capture by already existing particles. γ is a parameter that estimates the rate of capture of radicals by particles and droplets, and ζ is the ratio of the total latex volume to the volume of the aqueous phase. A_p is the ratio of the surface area of the polymer particles to the total latex volume:

$$A_p = \pi \, \mathrm{d}_p^2 N_p \tag{41}$$

The product ζA_m represents the micellar generation rate, where A_m is the area per volume of latex available to form micelles. It depends upon the soap concentration, its critical micelle concentration (CMC), and the soap coverage parameter α_s (which gives the amount of area covered by a molecule of soap). These parameters are available for many commercially available soaps. The area available for micellar particle generation also depends on A_p:

$$A_m = ([S] - [S]_{CMC}) \alpha_s - A_p \qquad A_m \geq 0 \tag{42}$$

As eq. (42) shows, A_m can be zero if the soap concentration does not exceed its CMC or if the soap must cover a large surface area already. Below the CMC, then, particles can only be generated via homogeneous mechanisms and then only if A_p is relatively small. In effect, this means that if polymer particles added or generated at the beginning of a process occupy a large surface area relative to the total latex volume, then particle generation

will cease early in the polymerization. All the soap present will be required to stabilize those polymer particles already formed.

Particle Size

Once $[M_p]$ and N_p have been determined, the emulsion particle size may be easily calculated. Since the polymer particles consist of both monomer and polymer, the model first computes the volume fraction of monomer in the particles

$$\phi_{m/p} = \frac{M_p \mathbf{M}_w}{\rho_m} \tag{43}$$

The total volume of the polymer phase is just

$$V_p = \frac{[P]V_l}{\rho_p (1 - \phi_{m/p})} \tag{44}$$

Dividing V_p by the total number of particles gives the average particle volume

$$v_p = \frac{V_p}{N_p V_l} \tag{45}$$

The root-mean-cube particle diameter is just

$$d_p = \left(\frac{6v_p}{\pi}\right)^{1/3} \tag{46}$$

Particle Size Distributions

The particle size distribution (PSD) is calculated in SCOPE by means of a histogram approach. Such an approach differs from more traditional methods, which calculate the leading moments of a distribution. The specific algorithm used in SCOPE applies to both semibatch and batch emulsion polymerizations. Particle size distributions produced in semibatch and continuous processes can be particularly intriguing, since particle nucleation and growth can both occur at the same time. If soap and initiator feed concentrations are manipulated, interesting multimodal particle size distributions can be formed.

First, SCOPE splits up the entire PSD into a finite number n_b of "bins"—typically, $n_b = 25$—covering the range of diameters from about 50 to about 10,000 Å. Each bin has a minimum diameter $D_{b,l}$ and a maximum diameter $D_{b,u}$ ($D_{b,u} = D_{b+1,l}$).

If polymer is added at the beginning of a process, the size distribution of the added polymer particles must be specified: the fraction of particles in each diameter bin $f_{b,i}$ must be known at the start. The initial concentration of polymer $[P]_i$, the $f_{b,i}$ and the bin diameters (the $d_{b,i}$) determine the total

number of particles present initially according to an equation similar to eq. (39):

$$N_i = \frac{[P]_i V_l}{\frac{\pi}{6} \rho_p \sum_{b=1}^{n_b} f_{b,i} d_{b,i}^3} \tag{47}$$

Once the distribution of the particles is known at time t, the kinetics of particle nucleation and growth taking place during the time increment $t \rightarrow t + 1$ determines the new distribution at time $t + 1$. The distribution can change in two ways: (1) through particle nucleation mechanisms, new particles can be generated, entering the lowest diameter bin ($b = 1$); or (2) by particle growth (or shrinkage) diameters of particles in bin b may increase or decrease and shift the distribution of these particles up to bin $b + 1$ or down to bin $b - 1$. Two parameters are used to describe distributional changes. One parameter is the diameter of new particles d_m. This minimum new particle diameter is usually between 50 and 300 Å, depending upon the soap used, the colloidal stability, and the degree of microcoagulation.[18] A second parameter q quantifies the relative growth rate of particles: particle growth is proportional to the diameter raised to the qth power. Thus, $q = 3$ if growth is proportional to volume, $q = 2$ if it is proportional to surface area.

If the distribution is known at time t, the distribution at time $t + 1$ can be calculated once the parameters q and d_m have been chosen. The algorithm for calculating the particle size distribution at time $t + 1$ given the particle size distribution at time t follows.

SCOPE first calculates the total number of particles generated in the time increment $(t, t + 1)$:

$$N_{\text{gen}} = N_{t+1} - N_t \tag{48}$$

Here N_t is calculated by an equation similar to eq. (47) (except that current diameters, number fractions, and polymer concentrations are used). Next, SCOPE calculates the total change in polymer particle volume

$$\Delta V_p = V_{p_{t+1}} - V_{p_t} \tag{49}$$

The model assumes that all freshly nucleated particles have a diameter d_m so that the volume of generated in this increment is

$$V_{\text{gen}} = \frac{\pi}{6} N_{\text{gen}} d_m^3 \tag{50}$$

Thus the volume remaining for growth (or shrinkage) is just

$$V_{\text{grow}} = \Delta V_p - V_{\text{gen}} \tag{51}$$

Since growth is proportional to some power q of the diameter, the volume of particles in bin b would be

$$V_{b',\,t+1} = V_{b,t} + V_{\text{grow}} \frac{d_{b,t}^q}{N_t \sum_{b=1}^{n_b} f_{b,t} d_{b,t}^q} \tag{52}$$

if $V_{\text{grow}} > 0$. Shrinkage can occur when the less dense monomer in the particles converts to the more dense polymer before new, fresh monomer is added. The new volume of bin b is related to the old volume by a shrinkage factor

$$V_{b',t+1} = V_{b,t} \frac{V_{p_{t+1}}}{V_{p_t}} \tag{53}$$

Now SCOPE calculates the new diameters in each bin b. [The primes used in eqs. (52) and (53) indicate that the particles in bin b at time t could have shifted to bin $b + 1$ or bin $b - 1$.] The new diameter to be expected for bin b (also primed) is

$$d_{b',t+1} = \left(\frac{6V_{b',t+1}}{\pi}\right)^{1/3} \tag{54}$$

The lowest diameter bin ($b = 1$) represents a special case, since it includes newly generated particles as well as those generated earlier and growing out. Thus its expected diameter must be recalculated according to

$$d_{1',t+1} = \frac{d_m N_{\text{gen}} + d_{1',t+1} N_{1',\text{t}}}{N_{t+1}} \tag{55}$$

The number fractions expected in each bin are calculated by evaluating

$$f_{b',t+1} = f_{t,b} \frac{N_t}{N_{t+1}} \qquad b \geq 2 \tag{56}$$

$$f_{1',t+1} = \frac{N_{\text{gen}} + N_{1',l}}{N_{t+1}} \qquad b = 1$$

Now SCOPE calculates the actual diameters and number fractions in each bin by determining the shift (if any) in the distribution. The upper and lower limits of the bin diameters are checked to see if the particles in bin b at time t have shifted to bin $b + 1$ or bin $b - 1$. We define the Kronecker $\delta_{bb'}$ such that

$$\delta_{bb'} = 1 \qquad \text{if } D_{b,l} \leq d_{b',t+1} < D_{b,u} \tag{57}$$

$$\delta_{bb'} = 0 \qquad \text{otherwise}$$

Then the actual fraction of particles in bin b at the new time $t + 1$ is

$$f_{b,t+1} = \sum_{b'=1}^{nb} f_{b',t+1}\, \delta_{bb'} \tag{58}$$

and the average diameter of the particles in bin b at time $t + 1$ is

$$d_{b,t+1} = \frac{\sum_{b'=1}^{nb} f_{b',t+1}\, \delta_{bb'}\, d_{b',t+1}}{f_{b,t+1}} \tag{59}$$

Copolymer Composition

To calculate copolymer compositions properly, it is necessary to consider many more elementary reactions than for homopolymerizations, which has been the focus of this paper up until now. For two monomers there are four propagation reactions and three termination reactions:

$$-M_1^{\cdot} + M_1 \xrightarrow{k_{p_{11}}} -M_1M_1^{\cdot}$$

$$-M_1^{\cdot} + M_2 \xrightarrow{k_{p_{12}}} -M_1M_2^{\cdot}$$

$$-M_2^{\cdot} + M_1 \xrightarrow{k_{p_{21}}} -M_2M_1^{\cdot}$$

$$-M_2^{\cdot} + M_2 \xrightarrow{k_{p_{22}}} -M_2M_2^{\cdot} \tag{60}$$

$$-M_1^{\cdot} + -M_1^{\cdot} \xrightarrow{k_{t_{11}}} -M_1 + -M_1 + \text{other products}$$

$$-M_1^{\cdot} + -M_2^{\cdot} \xrightarrow{k_{t_{12}}} -M_1 + -M_2 + \text{other products}$$

$$-M_2^{\cdot} + -M_2^{\cdot} \xrightarrow{k_{t_{22}}} -M_2 + -M_2 + \text{other products}$$

Technically each reaction listed has a different rate constant. Although all these rate constants may be known for certain well-studied two-monomer systems, systems containing three or more monomers involve many more such elementary reactions, making it difficult to treat copolymer systems rigorously.

Therefore, the SCOPE model makes several simplifications. First, only one k_t and usually only one k_p are used for most copolymer calculations in the model. As a rule, literature values of k_p and k_t for monomers in the recipe are (weighted) averaged to estimate these rate constants. Second, the model also assumes that the relative proportions of each monomer in the polymer particles are the same as those in the aqueous and droplet phases.

As stated earlier, experimental evidence supports the validity of this second assumption.[13,27,34] Third, the model assumes that the steady-state hypothesis for each type of radical is applicable. Finally, SCOPE assumes that tabulated reactivity ratios[35] or (if accurate reactivity ratios are not known) Price and Alfrey Q and e parameters[35-37] can provide reasonable estimates of relative reactivities.

For the specific case of two monomers, a more rigorous treatment can be used to calculate copolymer composition. Inspection of eqs. (30), (33), and (60) allows us to write the rates of propagation for two monomers:

$$R_{p_1} = \frac{N_p}{N_a}\left(k_{p_{11}}\,[\bar{n}_1]\,[M_{1p}] + k_{p_{12}}\,[\bar{n}_1]\,[M_{2p}]\right) \tag{61}$$

$$R_{p_2} = \frac{N_p}{N_a}\left(k_{p21}\,[\bar{n}_2]\,[M_{2p}] + k_{p_{22}}\,[\bar{n}_2]\,[M_{1p}]\right)$$

The average number of radicals per particle $\bar{n}$ is the sum of the average number ending in monomer M_1 and the average number ending in M_2 ($\bar{n} = \bar{n}_1 + \bar{n}_2$). Since the number of times an M_1 monomer unit follows an M_2 unit must be definition equal the number of times an M_2 unit follows an M_1 unit,

$$k_{p_{12}}\,\bar{n}_1\,[M_{2p}] = k_{p_{21}}\,\bar{n}_2\,[M_{1p}] \tag{62}$$

By using eq. (62) and $\bar{n}$ instead of $\bar{n}_1$ and $\bar{n}_2$, we obtain the results

$$R_{p_1} = \frac{\bar{n}N_p}{N_a}\;\frac{k_{p_{11}}\,k_{p_{22}}\,(r_{12}\,[M_{1p}]^2 + [M_{1p}]\,[M_{2p}])}{k_{p_{22}}\,r_{12}\,[M_{1p}] + k_{p_{11}}\,r_{21}\,[M_{2p}]} \tag{63}$$

$$R_{p_2} = \frac{\bar{n}N_p}{N_a}\;\frac{k_{p_{11}}\,k_{p_{22}}\,(r_{21}\,[M_{2p}]^2 + [M_{1p}]\,[M_{2p}])}{k_{p_{22}}\,r_{12}\,[M_{1p}] + k_{p_{11}}\,r_{21}\,[M_{2p}]}$$

Here r_{12} and r_{21} are the usual reactivity ratios defined by $r_{ij} = kp_{ii}/kp_{ij}$. Reactivity ratios are available for many common monomer pairs[34] or from Price-Alfrey Q and e values[34-37] using the equation

$$r_{ij} = \frac{Q_i}{Q_j}\exp\left[-e_i\,(e_i - e_j)\right] \tag{64}$$

Knowledge of the reactivity ratios and propagation rate constants allows us to calculate the instantaneous copolymer composition according to

$$F_1 = \frac{R_{p_1}}{R_{p_1} + R_{p_2}} = \frac{r_{12}f_1^2 + f_1f_2}{r_{12}f_1^2 + 2f_1f_2 + r_{21}f_2^2} \tag{65}$$

Here f_i denotes the mole fraction of monomer i in the residual monomer mix [calculated by using eqs. (10) for the current monomer concentration]. F_i is the mole fraction of copolymer formed at a particular instant. (Naturally, for two monomers $F_2 = 1 - F_1$.) The cumulative copolymer com-

position can be calculated by subtracting the amount of unreacted monomer of each type from the total amount added of that particular monomer.

For three or more monomers, calculating propagation rates for each monomer is quite involved.[13] In many cases key parameters (e.g., propagation rate constants of some of the monomers) are often not well known. Therefore, SCOPE computes a total propagation rate R_p. To do so, SCOPE uses an overall propagation rate constant k_p obtained by averaging the k_p values for each of the monomers in the system. SCOPE also uses mass-weighted-average values of the parameters $\mathbf{x}_c$ to calculate the monomer concentration in the particles $[M_p]$. Evaluation of the differential copolymer equation gives the ratio $F_i = R_{p_i}/R_p$ for each of the i monomers, so that individual propagation rates may at least be estimated. For three monomers the differential copolymer equation is

$$F_1 = \frac{a}{a + b + c}$$
$$F_2 = \frac{b}{a + b + c} \tag{66}$$
$$F_3 = \frac{c}{a + b + c}$$

where

$$a = f_1\left(\frac{f_1}{r_{13}r_{21}} + \frac{f_2}{r_{21}r_{32}} + \frac{f_3}{r_{31}r_{23}}\right)\left(f_1 + \frac{f_2}{r_{12}} + \frac{f_3}{r_{13}}\right)$$
$$b_2 = f_2\left(\frac{f_1}{r_{12}r_{31}} + \frac{f_2}{r_{12}r_{32}} + \frac{f_3}{r_{32}r_{13}}\right)\left(f_2 + \frac{f_1}{r_{21}} + \frac{f_3}{r_{23}}\right)$$
$$c = f_3\left(\frac{f_1}{r_{13}r_{21}} + \frac{f_2}{r_{23}r_{12}} + \frac{f_3}{r_{13}r_{23}}\right)\left(f_3 + \frac{f_1}{r_{31}} + \frac{f_2}{r_{32}}\right)$$

Terpolymers involves six reactivity ratios. Differential copolymer equations for more than three monomers are complicated expressions involving many reactivity ratios (some of which are known with little accuracy). Thus, although eqs. (66) could be used to solve for the instantaneous copolymer compositions for three monomers, SCOPE allows the option of using the following m-monomer differential copolymer equation for three or more monomers:

$$F_i = \frac{f_i Q_i \sum_{k=1}^{m} [f_k Q_k \exp(-e_i e_k)]}{\sum_{j=1}^{m} f_j Q_j \sum_{k=1}^{m} [f_k Q_k \exp(-e_j e_k)]} \tag{67}$$

Equation (67) uses monomeric Q and e values, which have been determined and tabulated[35-37] for hundreds of monomers. To calculate the approximate

propagation rates for each monomer used in eqs. (10), SCOPE multiplies the overall propagation rate by the F_i : $R_{p_i} = R_p F_i$.

Molecular Weight

The molecular weight of a (co)polymer formed by emulsion polymerization is determined by the underlying kinetic mechanisms: propagation, termination (by either combination or disproportionation), and/or transfer reactions to species present in the polymerizing mixture. Usually one or two mechanisms dominate to control molecular weight. This is the termination or transfer reaction that is fastest relative to propagation. High-molecular-weight polymer is formed when propagation reactions are rapid relative to all transfer and termination reactions. Low-molecular-weight polymer can then be formed by addition of a mercaptan, which usually have high transfer rate constants.

First consider transfer reactions involving a particular transfer agent T. The material balance equation can, of course, be used to determine the concentration of T. The rate of chain transfer depends upon the concentration of T in the polymer particles:

$$R_{tr-T} = k_{tr-T} [T_p] [M\cdot] = \frac{k_{tr-T} [T_p] \bar{n} N_p}{N_a} \tag{68}$$

Many chain transfer agents are long-chain organic molecules (e.g., mercaptans), so the SCOPE model assumes T is exclusively in the organic phase (none at all in the aqueous phase). Thus,

$$[T_p] = [T] \frac{V_l}{V_o} \tag{69}$$

Where V_o is the total volume of organic (monomer + polymer) phase, including both the monomer droplets and the polymer particles.

Besides transfer to a chain transfer agent, the molecular weight could be controlled or influenced by transfer to monomer. The rate of transfer to monomer i is

$$R_{tr-M_i} = \frac{k_{tr-M_i} [M_{i_p}] \bar{n} N_p}{N_a} \tag{70}$$

Chain transfer rate constants for various monomers, the k_{tr-M_i}, often expressed as a fraction of the propagation rate constant k_p, are available from Ref. 38. $[M_{i_p}]$ is the concentration of monomer i in the particles.

Termination reactions also influence the molecular weight distribution. As eqs. (34) indicate, termination by combination would appear to produce more lower molecular weight polymer than termination by disproportionation. The rate of termination by disproportionation is

$$R_{td} = k_{td} [M\cdot]^2 = \frac{k_{td} \bar{n}^2 N_p^2}{N_a^2} \tag{71}$$

Similarly, the rate of termination by combination is

$$R_{t_c} = k_{t_c} [M\cdot]^2 = \frac{k_{t_c} \bar{n}^2 N_p^2}{N_a^2} \tag{72}$$

Still other reactions can influence the molecular weight distribution in emulsion (co)polymers, including transfer-to-polymer reactions and terminal double-bond polymerizations. Such reactions can produce chain branching in polymer molecules (see, for example, the discussion in Ref. 33 on vinyl acetate). On the other hand, these reactions are unimportant for many monomers. Expressions for calculating molecular weight when terminal double-bond and transfer-to-polymer reactions are important are currently being developed and will be reported in a future publication.

Neglecting transfer-to-polymer and terminal double-bond polymerization reactions simplifies molecular weight calculations considerably. The rates of termination and transfer are simply compared with the overall propagation rate. Following the usual treatment,[13,39] SCOPE calculates two ratios

$$\begin{aligned} z_1 &= \frac{R_{tr-T} + R_{t_d} + \sum_{i=1}^{m} R_{tr-M_i}}{R_p} \\ z_2 &= \frac{R_{t_c}}{R_p} \end{aligned} \tag{73}$$

which determine the instantaneous molecular weight distribution according to[39]

$$w(r) = \frac{r(z_1 + z_2)}{(1 + z_1 + z_2)^r} \left[z_1 + \frac{z_2(z_1 + z_2)^r}{2} \right] \tag{74}$$

where $w(r)$ is the probability of finding a polymer chain of length r. The instantaneous number-average molecular weight is

$$\overline{\mathbf{M}}_N = \frac{\mathbf{M}_w}{z_1 + \frac{z_2}{2}} \tag{75}$$

and the instantaneous weight average molecular weight is

$$\overline{\mathbf{M}}_W = 2\mathbf{M}_w \frac{z_1 + \frac{3z_2}{2}}{(z_1 + z_2)} \tag{76}$$

where $\mathbf{M}_w$ is the average monomer molecular weight. When termination by combination is relatively slow with respect to other transfer and termination reactions, the polydispersity ratio $\overline{\mathbf{M}}_W/\overline{\mathbf{M}}_N = 2$, when it dominates, $\overline{\mathbf{M}}_W/\overline{\mathbf{M}}_N = 1.5$.

Since the quantities computed in eqs. (74) through (76) are instantaneous,

the cumulative molecular weight distribution is calculated by integrating $w(r)$ over the weight of polymer formed in the time increment $(t, t + 1)$ and then computing cumulative number and weight averages. Typically, the molecular weight distribution broadens during a batch or semibatch polymerization, and this is reflected in a cumulative polydispersity index that slowly increases above 2.

NUMERICAL METHOD

A FORTRAN computer program solves the differential and algebraic equations given in previous sections. This computer program allows the user to enter into a file the emulsion recipe, flow rates, temperatures, rate constants, and physical property parameters. The program then solves the equations developed in these sections to calculate species concentrations, temperatures, and polymer properties as a function of time. The differential system simulator, version 2 (DSS/2) package from Lehigh University,[40] which provides the option of using 16 different numerical algorithms, solves the coupled differential equations. Typically, Gear's algorithm[41] is used with an error tolerance of approximately 0.001 and a constant time step of 1 s. The constant time step is required because the control equation (19) must be evaluated at equally spaced time intervals. A typical simulation run requires 10 s on an IBM 3081 computer. (An additional 20 s is usually required to calculate detailed particle size distributions and molecular weight distributions.)

GLOSSARY

a_1	Constant (usually determined from experiments) used to calculate change in radical efficiency as a function of initiator concentration
a_2	Constant (usually determined from experiments) used to calculate the partitioning of monomer in the aqueous phase
a_i	Constants (usually determined from experiments) used to track the change in termination rate as a function of conversion (i = 3 and 4)
$[A]$	Activator concentration, mol/m^3
A_h	Area available for heat transfer, m^2
A_m	Area (per volume of latex) available for micellar particle generation, m^{-1}
A_p	Area (per volume of latex) occupied by all polymer particles, m^{-1}.
A_x	Arrhenius pre-exponential factor for rate constant k_x, ($x = d, p, r_1, r_2, t$), m^3/(mol-s) or (if $x = d$), s^{-1}
b	Subscript indicating a particular particle size diameter range (bin)
$[C]$	Catalyst concentration, mol/m^3
C_{px}	Heat capacity (x = 1, *ef* or *w* or *s*), J-kg/K
C_x	Current controller output, pct
d_m	New particle diameter, m
d_p	Diameter of a polymer particle, m

d_r	Reactor diameter, m
$d_{b,i}$	Diameter of particles initially present in bin b, m
$d_{b,t}$	Diameter of particles in bin b at time t, m
$D_{b,l}$	Minimum diameter of particles in bin b, m
$D_{b,u}$	Maximum diameter of particles in bin b, m
D_x	Deriviative constant for a PID controller
e	Dimensionless error (deviation from set-point temperature)
ef	Subscript indicating monomer emulsion feed
e_i	e value for monomer i (see section on copolymer composition)
E_x	Activation energy for rate constant x ($x = d, p, r_1, r_2, t$), J/mol
f	Radical efficiency factor
f_0	Radical efficiency factor at the reference initiator concentration $[I_0]$
f_i	Mole fraction of monomer i in the residual monomer mixture
$f_{b,i}$	Fraction of particles initially present in bin b
$f_{b,t}$	Fraction of particles in bin b at time t
F_{ef}	Monomer emulsion flow rate, m^3/s
F_i	Mole fraction of monomer i in the instantaneous copolymer
F_w	Cooling water flow rate, m^3/s
h_r	Reactor height, m
ΔH_{p_i}	Heat of polymerization of monomer i, J/kg
i	Subscript indicating an initial condition
i	Subscript indicating the ith element of a set
in	Subscript indicating inlet
$[I]$	Initiator concentration, mol/m^3
$[I_0]$	Reference initiator concentration (where $f = f_0$), mol/m^3
I_x	Reset constant for a PID controller
k'_{de}	Rate constant parameter for radical desorption, $m^2/(mol\text{-}s)$
k_d	Decomposition rate constant, s^{-1}
k_p	Propagation rate constant, $m^3/(mol\text{-}s)$
$k_{p_{ij}}$	Rate constant for propagation of monomer i with polymer radical j, $m^3/(mol\text{-}s)$
k_{r_1}	Redox initiation rate constant, $m^3/(mol\text{-}s)$
k_{r_2}	Redox initiation rate constant, $m^3/(mol\text{-}s)$
k_{tc}	Rate constant for termination by combination, $m^3/(mol\text{-}s)$
k_{t_d}	Rate constant for termination by disproportionation, $m^3/(mol\text{-}s)$
k_{tr-x}	Rate constant for chain transfer to species x ($x = M_i, T$), $m^3/(mol\text{-}s)$
l	Subscript indicating latex
m	Subscript indicating monomer
m	Total number of monomers in the system
$[M\cdot]$	Concentration of polymer radicals, mol/m^3
M_i	Molecular weight of monomer i, kg/mol
$[M_i]$	Concentration of monomer i, mol/m^3
$[M_{ip}]$	Concentration of monomer i in the polymer particles, mol/m^3
$[M_p]$	Concentration of monomer in the polymer particles, mol/m^3
$[M_p]_{sat}$	Saturation concentration of monomer in the particles, mol/m^3
$[M_{ta}]$	Concentration of total monomer added, kg/m^3

$\mathbf{M}_w$	Average monomer molecular weight, kg/mol
$\overline{\mathbf{M}}_N$	Instantaneous number-average molecular weight of polymer
$\overline{\mathbf{M}}_W$	Instantaneous weight-average molecular weight of polymer
$\overline{\mathbf{n}}$	Average number of radicals per particle
n_b	Total number of bins for the particle size distribution
N_a	Avogadro's number, 6.02×10^{23}
N_{gen}	Number of particles generated in time increment $(t, t + 1)$
N_p	Particle concentration, m^{-3}
$N_{p_{\text{gen}}}$	Particle generation rate, $\text{m}^{-3}\ \text{s}^{-1}$
N_{p_i}	Initial polymer particle concentration, m^{-3}
N_t	Total number of particles in the latex at time t
o	Subscript indicating organic phase
p	Subscript indicating polymer or propagation
$p_i^{(0)}$	Some property (e.g., density) of a component in its pure form
$\mathbf{P}$	Mass-weighted-average of some property (e.g, density)
$[P]$	Concentration of polymer, kg/m^3
P_r	Dead polymer of chain length r
p_x	Proportional band (including the action) of a PID controller
q	Exponent indicating relative growth rate for polymer particles (see section on particle size distribution)
Q_i	Q value for monomer i (see section on copolymer composition)
r	Subscript indicating chain length
r_{ij}	Reactivity ratio $(=kp_{ii}/kp_{ij})$ for monomers i and j
$[R\cdot]$	Concentration of primary (initiator) radicals, mol/m^3
R_p	Rate of propagation, $\text{mol/(m}^3\text{-s)}$
R_{p_i}	Rate of propagation for monomer i, $\text{mol/(m}^3\text{-s)}$
R_r	Dead polymer of chain length r
$R_r^{\cdot}$	Live polymer of chain length r
R_{t_c}	Rate of termination by combination, $\text{mol/(m}^3\text{-s)}$
R_{td}	Rate of termination by disproportionation, $\text{mol/(m}^3\text{-s)}$
R_{tr-M_i}	Rate of transfer to monomer i, $\text{mol/(m}^3\text{-s)}$
R_{tr-T}	Rate of transfer to chain transfer agent, $\text{mol/(m}^3\text{-s)}$
R_A	Rate of reaction of activator, $\text{mol/(m}^3\text{-s)}$
R_C	Rate of reaction of promoter, $\text{mol/(m}^3\text{-s)}$
R_I	Initiation rate, $\text{mol/(m}^3\text{-s)}$
R_T	Rate of reaction of chain transfer agent, $\text{mol/(m}^3\text{-s)}$
sp	Subscript indicating set point
$[S]$	Soap concentration, mol/m^3
$[S]_{\text{CMC}}$	Soap critical micelle concentration, mol/m^3
S_x	Value stem position corresponding to valve x ($x = ef$ or w), pct
t	Current time, s
t	Subscript indicating the current time
$t + i$	Subscript indicating the value of the subscripted variable at the ith future time step
$t - i$	Subscript indicating the value of the subscripted variable at the ith previous time step
tr	Subscript indicating chain transfer
t_w	Cooling water jacket thickness, m

T	Temperature, K
$[T]$	Chain-transfer agent concentration, mol/m^3
T_{meas}	Measured reactor (latex) temperature, K
T_{ref}	Reference temperature for the latex, K
$[T_p]$	Concentration of chain transfer agent in the polymer particles, mol/m^3
T_x	Temperature (x = 1, *ef*, *w*, *sp*, or *i*), K
U	Heat transfer coefficient, J/(m^2-s-K)
v_p	Volume of a polymer particle, m^3
V_{gen}	Volume of particles generated in time increment (t, t + 1), m^3
V_l	Latex volume, m^3
V_o	Volume of organic phase, m^3
V_p	Total volume of polymer particles, m^3
w	Subscript indicating cooling water
$w(r)$	Instantaneous probability of finding a polymer chain of length r
w_i	Weight fraction of ith component
x_c	Critical conversion (conversion at which the monomer droplets disappear)
X	Weight conversion
z_1	Ratio used in calculating the molecular weight distribution
z_2	Ratio used in calculating the molecular weight distribution
ρ_x	Density of component x, kg/m^3
$\delta_{bb'}$	Kronecker delta (see section on particle size distribution)
a_s	Area covered per mole of soap, m^2/mol
γ	Rate of radical capture by particles (dimensionless parameter)
ζ	Ratio of latex volume to the aqueous phase volume
τ_x	Time constant for device x (x = *ef*, *w*, or meas), s
μ	Rate constant parameter for homogeneous particle nucleation, m^{-1}
$\phi_{p/m}$	Monomer volume fraction in the particles
π	3.14159

The author would like to thank the Rohm and Haas Company for supporting this work. He also gratefully acknowledges discussion with Professor John MacGregor of McMaster University, Dr. Geoff Smith, Dr. Ed Firouztale, Mr. Bob Thompson, and Mr. Jeff Nathanson of Rohm and Haas.

References

1. W. D. Harkins, *J. Amer. Chem. Soc.*, **69**, 1428 (1947).
2. W. F. Smith and R. H. Ewart, *J. Chem. Phys.*, **16**, 592 (1948).
3. W. H. Stockmayer, *J. Polym. Sci.*, **24**, 314 (1957).
4. J. T. O'Toole, *J. Appl. Polym. Sci.*, **9**, 1291 (1965).
5. J. L. Gardon, *J. Polym. Sci., Part A-1*, **6**, 623, 643, 665, 687, 2853, 2859 (1968).
6. J. Ugelstad, P. C. Mork, and J. E. Aasen, *J. Polym. Sci., Part A-1*, **5**, 2281 (1969).
7. W. J. Priest, *J. Phys. Chem. (Ithaca)*, **56**, 1077 (1952).
8. J. H. Baxendale, M. G. Evans, and J. K. Kilham, *Trans. Faraday Soc.*, **42**, 668 (1946); J. H. Baxendale, S. Bywater, and M. G. Evans, *Trans. Faraday Soc.*, **42**, 675 (1946).
9. C. P. Roe, *Ind. Eng. Chem.*, **60**, 20 (1968).
10. R. M. Fitch, M. B. Prenosil, and K. J. Sprick, *J. Polym. Sci., Part C*, **27**, 95 (1969); R. M. Fitch, *Polymer Colloids*, Pergamon Press, New York, 1971; R. M. Fitch, in *Emulsion Polymers*

and Emulsion Polymerization, D. R. Bassett and A. E. Hamielec, Eds., *ACS Symp. Ser.,* **165**, 1 (1981).

11. J. G. Brodynan, J. A Cala, T. Konen, and E. L. Kelley, *J. Colloid Sci.,* **18**, 73 (1963).
12. K. W. Min and W. H. Ray, *J. Macromol. Sci., Rev. Macromol. Chem.,* **C11**, 177 (1974); *J. Appl. Polym. Sci.,* **22**, 89 (1978).
13. A. E. Hamielec and J. F. MacGregor, Polymer Reaction Engineering, Notes for a short course at McMaster University, Hamilton, Ontario, Canada, 1982; in *Polymer Reaction Engineering,* K. H. Reichert and W. Geisler, Eds., Hanser, Berlin, 1983, pp. 21–72.
14. E. Firouztale and E. P. Dougherty, to be published.
15. M. Nomura, K. Yamamoto, I. Horie, K. Fujita, and M. Harada, *J. Appl. Polym. Sci.,* **27**, 2483 (1982).
16. R. G. E. Franks, *Mathematical Modeling in Chemical Engineering,* Wiley, New York, 1979.
17. D. C. Blackley, *Emulsion Polymerization,* Wiley, New York, 1975.
18. G. Lichti, R. G. Gilbert, and D. H. Napper, *J. Polym. Sci., Polym. Chem. Ed.,* **21**, 269 (1974).
19. T. W. Hoffmann, Application of fundamental concepts: The modeling of emulsion copolymerization reactors, unpublished manuscript, McMaster University, Hamilton, Ontario, Canada, 1982.
20. E. Hakoila, *Ann. Univ. Turk., Ser. A,* **66**, 7 (1963).
21. Y. I. Yelisejeva, in *Emulsion Polymerization,* I. Piirma, Ed., Academic Press, New York, 1982.
22. I. M. Kolthoff and I. K. Miller, *J. Amer. Chem. Soc.,* **73**, 3055 (1951).
23. M. Morton, S. Kaizerman, and M. W. Altier, *J. Colloid Sci.,* **9**, 300 (1954).
24. W. R. Kriegbaum and D. K. Carpenter, *J. Polym. Sci.,* **14**, 241 (1954).
25. T. Oishi and J. M. Prausnitz, *Ind. Eng. Chem., Chem. Proc. Des. Develop.,* **17**, 330 (1978).
26. A. Fredenslund, R. L. Jones, and J. M. Prausnitz, *AIChE J.,* **21**, 1086 (1975).
27. R. G. Fordyce and E. C. Chapin, *J. Amer. Chem. Soc.,* **69**, 581 (1947).
28. P. G. deGennes, *J. Chem. Phys.,* **55**, 572 (1971); *Scaling Concepts in Polymer Physics,* Cornell University, Ithaca Press, New York, 1979; M. Tirrell, private communication, 1984.
29. S. K. Soh and D. C. Sundberg, *J. Polym. Sci.,* **20**, 1345 (1982).
30. F. L. Marten and A. E. Hamielec, *ACS Symp. Ser.,* **104**, 43 (1979).
31. C.-C. Lin and Y.-O. Wang, *J. Appl. Polym. Sci.,* **26**, 3909 (1981).
32. J. Ugelstad, P. C. Mork, P. Dahl, and P. Ragnes, *J. Polym. Sci., Part C,* **27**, 49 (1969).
33. C. Kiparissides, J. F. MacGregor, and A. E. Hamielec, *J. Appl. Polym. Sci.,* **23**, 401 (1979).
34. A. J. Seiner, *J. Polym. Sci.,* **A3**, 2401 (1965).
35. T. Alfrey, Jr., and C. C. Price, *J. Polym. Sci.,* **2**, 101 (1947).
36. T. Alfrey, J., J. J. Bohrer, and H. Mark, *Copolymerization,* Wiley Interscience, New York, 1952, Chaps. III and IV.
37. R. K. S. Chang and V. E. Meyer, *J. Polym. Sci.,* **C25**, 11 (1968).
38. J. Brandup and E. H. Immergut, *Polymer Handbook,* Wiley, New York, 1975.
39. J. Balke, Ph.D. thesis, McMaster University, Hamilton, Ontario, Canada, 1974.
40. W. E. Schiesser, The differential systems simulator (DSS/2), unpublished computer program, Lehigh University, Bethlehem, Pennsylvania, 1981.
41. C. W. Gear, *ACM Commun.,* **14**, 176 (1971).

Received September 19, 1985
Accepted October 5, 1985